Moisture Transport in Wood-Based Structural Panels under Transient Hygroscopic Conditions

Daniel Way
Frederick A. Kamke
Arijit Sinha

Abstract

Development of moisture gradients within wood and wood-based composites can result in irreversible moisture-induced damage. Accelerated weathering (AW), generally employing harsh environmental conditions, is a common tool for assessing moisture durability of wood composite products. Use of milder AW conditions, such as cyclic changes in relative humidity (RH), may be of interest to the wood-based composites industry in assessing moisture durability under more realistic conditions. The primary objective of this study was to determine whether moisture profile development in oriented strand board and plywood during cyclic RH changes could be reasonably predicted with a simple moisture transport model, which may be practical for wood-based composite industry members seeking to develop new AW protocols. The diffusion model based on Fick's second law with empirically determined moisture transport parameters fits the experimental data reasonably well for the purpose of screening RH parameters.

As hygroscopic materials, wood-based composites exchange moisture with the surrounding environment. Rapid changes in external conditions or differing climates on opposing faces lead to moisture gradient formation within the cross section, potentially causing product damage and mechanical property losses. Accelerated weathering (AW) is a common method to assess and compare moisture durability of wood composite products. Performed in the laboratory setting following standardized or custom procedures, AW allows for product comparison, product durability assessment, and postmanufacturing validation of compliance standards performance. The ''accelerated'' portion originates from the need to expedite potential degradation and leads to the use of severe conditions such as hot water soaking, boiling, steaming, vacuum-pressure soaking, freezing, and high temperature drying (e.g., APA 2011, ASTM International 2012). While useful for assessing and comparing product performance, AW conditions are more severe than conditions to which products may be exposed to during service (River 1994, Saad et al. 2016).

More accurate depictions of moisture durability attributes in service could potentially be gained from use of milder AW conditions, such as cyclic relative humidity (RH) changes (Moya et al. 2009, Saad et al. 2016). Optimizing an AW method for each set of potential environmental conditions and sampling schemes is time and resource intensive. Tailoring AW procedures to produce the largest moisture gradients along with determining optimum sampling times would benefit from the availability of a model capable of reasonably predicting when and where the largest moisture gradients are likely to occur based on the moisture transport properties of the product of interest and the imposed environmental conditions. The primary objective of this study was to determine whether moisture profiles in oriented strand board (OSB) and plywood during cyclic RH changes could be reasonably predicted with a simple moisture transport model, which may be practical to wood-based composite industry members interested in implementing less severe moisture durability assessment procedures. Moisture transport properties required for the model were empirically determined using readily available equipment.

The authors are, respectively, Product Engineer, Boise Cascade Co., White City, Oregon (waydaj@gmail.com); and Professor and JELD-WEN Chair of Wood-based Composites Science (Fred.Kamke@oregonstate.edu) and Associate Professor of Renewable Materials (Arijit.Sinha@oregonstate.edu [corresponding author]), Dept. of Wood Sci. and Engineering, Oregon State Univ., Corvallis.
This paper was received for publication in March 2020. Article no. 20-00012.

Forest Prod. J. 70(3):283–292.
doi:10.13073/FPJ-D-20-00012

Materials and Methods

Moisture transport model background

Fick's laws have been applied to describe the diffusion of moisture in wood and wood-based products, with Fick's second law describing unsteady-state diffusion (Siau 1995a). Concerns over the ability of Fick's law to adequately depict moisture transport have been raised, since no separation between bound water and water vapor diffusion is considered. Other peculiarities, such as slow sorption and thickness-dependent diffusion coefficients, also lead to deviations from Fick's law (Wadsö 1993). More sophisticated and subsequently more physically accurate methods employing multiphase, or multi-Fickian, techniques allow for consideration of the coupling between bound water and water vapor diffusion (Frandsen et al. 2007, Eitelberger and Hofstetter 2011). Despite the physically inaccurate driving force assumptions posed by Fick's law, researchers have used it to model moisture transport in wood (Gereke 2009, Saft and Kaliske 2011, Hassani et al. 2016, Niklewski et al. 2016) and wood-based composites (Wu and Suchsland 1996, Ganev et al. 2005), achieving reasonable agreement with experimental data through a relatively simplistic numerical scheme.

As outlined by previous authors (Cai and Avramidis 1997, Olek et al. 2005, Shi 2007, Niklewski et al. 2016), the partial differential equation describing isothermal unsteady-state diffusion of moisture in one dimension according to Fick's law is:

$$\frac{\partial C}{\partial t} = \frac{\partial}{\partial x}\left(D\frac{\partial C}{\partial x}\right) \tag{1}$$

where C is the moisture concentration (kg m^{-3}), t is time (s), x is the distance from the centerline of a symmetrical specimen in the direction of moisture flow (m), and D is the diffusion coefficient (m^2 s^{-1}). The initial moisture concentration across the domain is frequently assumed to be uniform and the boundary conditions specified as:

$$-D\frac{\partial C}{\partial x} = S\Big(C(x,t) - C_\infty\Big) \qquad (x,t) \in \Gamma(\pm a, t) \tag{2}$$

where S is the surface emission coefficient (m s^{-1}), C_∞ is the equilibrium moisture concentration of the solid within the surrounding air, Γ is the boundary surface, and a is the specimen half thickness. The moisture concentration dependence of the diffusion coefficient has been estimated by fitting an exponential function of the form (Wu and Suchsland 1996, Olek et al. 2005):

$$D(C) = D_0 \cdot \exp(\alpha \cdot C) \tag{3}$$

where D_0 (m^2 s^{-1}), and α (m^3 kg^{-1}) are coefficients determined by nonlinear least squares regression.

Material

OSB and plywood were selected for this study due to their wide use in residential construction in the United States. Commercial OSB of 11.1 mm nominal thickness was purchased from a local building supply store. The panels possessed an APA span-rating of 24/16 and were rated *Exposure 1*, meaning they were intended to resist the effects of moisture due to temporary exposure during construction (APA 2018). Correspondence with the manufacturer revealed that the three-layer boards were primarily produced from aspen (*Populus* sp.) strands with the remainder composed of assorted hardwoods. Phenol-formaldehyde (PF) adhesive was used in the faces, and polymeric diphenylmethane diisocyanate (pMDI) adhesive in the core. The weight-based shelling ratio and wax loading were approximately equal throughout the layers.

Plywood for this study was produced in the laboratory. Four-ply construction was used for the panels where the two outer layers were aligned parallel to each other and orthogonal to the two inner plies. The Douglas-fir (*Pseudotsuga menziesii*) veneer was radially peeled to 3.18-mm nominal green thickness, dried, and sorted at a plywood manufacturer's facility. Only heartwood veneer with minimal visual defect was selected. Each plywood panel (0.61 m wide by 1.22 m long) was produced from a single veneer sheet (1.22 m wide by 2.44 m long) to minimize variation throughout the panel. Commercial PF plywood resin was applied with a hand roller at a spread rate of 0.15 kg/m^2 of glue line per the manufacturer's recommendation. The location of visual defects in each veneer was marked on the top sheet for avoidance during final specimen preparation. Panels were hot-pressed to 11.9-mm target thickness until the center glue line reached curing temperature for 2 minutes. Twelve panels were produced in total.

Sorption specimens.—Previous work showed that OSB (Timusk 2008) and other mat-formed composites (Wu and Suchsland 1996, Ganev et al. 2003) do not perform as homogenous uniform materials in terms of moisture transport, with properties differing between face and core layers. Therefore, the face and core regions were isolated for investigation. Twenty 305 by 305-mm pieces were removed from the OSB panels in the as-received state. Three 50 by 50-mm pieces were removed in an adjacent region of the original panel to determine density profile through the thickness using an X-ray densitometer (Quintek Measurement Systems, Inc., Knoxville, Tennessee; Model QDP-01X). The intersecting points of the actual density profile and the average density for the entire profile were considered an approximation of the position in which the two face layers and the core layer were located. The 305 by 305-mm pieces were then run through a knife planer, following the methodology of Timusk (2008). Along with the density scan data, location of the face and core layers was further refined based on the position in which the strand orientation and size was consistent between two passes. All face specimens included the smooth surface of the OSB panel. Average thickness of the 305 by 305-mm pieces after planing was 2.7 and 4.0 mm for the face and core, respectively, which were then cut into 75 by 75-mm specimens for sorption experiments. Average ovendry (OD) density was 698 ± 64 and 532 ± 29 kg m^{-3} for face and core specimens, respectively.

Diffusion coefficients of wood and adhesive can vary significantly (Sonderegger et al. 2010, Mannes et al. 2014), so D was determined for veneer and adhesive separately. Both veneer and adhesive were obtained from the same processing batch as those used in plywood panel production. Clear specimens measuring 75 by 75 mm were cut from six veneer sheets for use in unsteady sorption experiments, with 580 ± 84 kg m^{-3} OD density. A modified cup method was used to estimate the adhesive diffusion coefficient (D_{adh}) where 10 clear 152 by 152-mm sheets were laser cut into four 67-mm-diameter specimens per sheet. Two of the four

pieces obtained per sheet were selected for the control group, while the other two were used for the bonded group. An adhesive layer was applied with a brush to one of the veneer disks in the bonded group, and the two disks were hot-pressed together at the same target compression as the plywood panels until the bondline reached cure temperature for 2 minutes. The procedure was repeated for the control group in the absence of adhesive.

Sorption experiments.—Climatic conditions during sorption experiments were regulated in a climate chamber with good air circulation that was capable of maintaining temperature at ± 0.5°C and RH at ±1.0 percent. All sorption experiments were performed under isothermal conditions at 25°C. Sorption isotherms were determined with 10 replications of OSB face, OSB core, and veneer. Equilibrium moisture content (EMC) was determined by collecting the mass of each specimen after reaching equilibrium at each RH level, which was defined as less than a 0.1 percent change in mass over 24 hours. The RH conditioning scheme was 30 → 45 → 60 → 75 → 90 → 75 → 60 → 45 → 30 percent.

Nelson (1983) developed a sorption model based on Gibbs free energy to describe Type II sorption behavior of cellulosic materials, which has been used to quantify sorption behavior of solid wood (Nelson 1983), particle board (Wu and Suchsland 1996), and OSB (Wu and Ren 2000). Experimental data at each EMC were fit to the inverse form of Nelson's model to estimate coefficients M_v and A following the methodology of Wu and Ren (2000):

$$\mathrm{EMC} = M_v\left\{1.0 - \frac{1}{A}\ln\left[\left(-\frac{R\cdot T}{W_w}\ln(\mathrm{RH})\right)\right]\right\} \quad (4)$$

where RH is relative humidity (fractional), W_w is molecular weight of water (18 g mol^{-1}), R is universal gas constant (8.314 J mol^{-1} K^{-1}), T is temperature (K), A is natural logarithm of Gibbs free energy per gram of sorbed water as RH approaches zero (J g^{-1}), and M_v is a material constant approximating the fiber saturation point for desorption, fractional form (Wu and Ren 2000).

Moisture transport coefficient determination.—Transient sorption experiments were performed by subjecting specimens at equilibrium to a sudden change in RH and periodically measuring mass (±0.01 g) until equilibrium was attained. The procedure was performed over four steps in both adsorption and desorption at 25°C according to the RH conditioning scheme used for sorption isotherm determination. Five replications of each material type were evaluated. One-dimensional moisture transport through the thickness direction (radial direction for veneer and radial/tangential direction for OSB) was achieved by applying silicone to the edges. A theoretical solution to Equation 1 (Crank 1986) based on the fractional moisture concentration change over each sorption was used to extract the optimal pair of D and S from unsteady sorption experiments using a nonlinear simplex procedure to minimize the objective function (Eq. 5) as previously described by other authors (Cai and Avramidis 1997, Shi 2007). Detailed information on the specific procedure used is available elsewhere (Way 2018).

$$F = \frac{\sum_{i=1}^{N}\left[E_{\exp}(t_i) - E_{\mathrm{pred}}(t_i)\right]^2}{N} \quad (5)$$

where E is the fraction moisture concentration change over each sorption step at time t_i for the measured value (exp) and that predicted by the theoretical solution (pred), and number of data points N.

The steady-state wet cup method was used to estimate D_{adh} where RH inside the cup was maintained at 84 percent (EMC 12.9% ± 0.31%) with a KCL saturated salt solution and 30 percent (EMC of 4.42% ± 0.32%) outside the cups via conditioning chamber maintained at 30°C and 30 percent RH. Steady state was considered when slope of mass loss versus time curve differed less than 2 percent over 168 hours. Approximating D_{adh} requires knowledge of the bondline thickness and the concentration difference across the bondline. Measuring both of these properties is difficult, since the bondline thickness varies depending on the local wood structure, and measuring the concentration difference across the bondline requires nondestructive measurements. In estimating D_{adh}, a continuous bondline thickness of 0.15 mm and an MC difference of 1.3 percent corresponding to a 7 kg m^{-3} difference across the bondline were assumed, both of which were considered conservative estimates based on previous work (Sonderegger et al. 2010, Mannes et al. 2014). A steady-state moisture flux equation was used to estimate D_{adh}, which is described in detail elsewhere (Way 2018).

Moisture transport model implementation.—One-dimensional moisture transport was modeled based on Equations 1 to 3 and implemented via the finite element method in COMSOL Multiphysics (COMSOL 2015a). Symmetry about the middle thickness of each material type was assumed. Dimensional changes resulting from shrinkage and swelling were neglected. Isothermal conditions of 25°C were assumed, and changes in localized temperature due to phase changes were neglected. Temperature plays an important role in the moisture transfer process, and while experiments in this study were performed under isothermal conditions, an Arrhenius-type expression has been used by others to describe the global temperature dependency on the diffusion coefficient (Niklewski et al. 2016).

The OSB domain consisted of two discrete, homogenous sections—the face and core material. Each subdomain was set to 2.8 mm thick based on density scans of the OSB. The different face and core densities required specification of two additional conditions at their interface: (1) the moisture flux across the interface was assumed equal and (2) the concentration of each region at the interface corresponded to the same MC (Wu and Suchsland 1996). The plywood domain consisted of two veneers abruptly separated by a bondline. Thickness was set to 3.1 mm for each veneer and 0.15 mm for the adhesive layer. It was assumed that moisture flux was equal and continuity in MC was present at the interface between the veneer and bondline. Since adhesive sorption behavior was unknown, it was assumed that the adhesive had reached the same MC levels as the veneer, which was found to coincide reasonably well for phenol resorcinol–formaldehyde (PRF) adhesive films (Wimmer et al. 2013).

Mesh size was refined until the difference in output value differed by less than 1 percent, which corresponded to a physical mesh size of approximately 0.15 mm for both OSB and plywood. COMSOL Multiphysics automatically adjusts the time steps to take the maximum step possible at a specified convergence tolerance based on phenomena

occurring within the model (COMSOL 2015b). On average, 105 time steps were required to solve the model.

Experimental procedure for model comparison.—Experimental data for evaluating model performance were generated by subjecting full thickness OSB and plywood specimens (75 by 75 mm) to three RH cycles. Each cycle consisted of a high and low step at 25°C, both of 24-hour duration, in the same climate chamber used for component sorption tests. The high and low RH set points were 90 and 30 percent, respectively. Specimen edges were sealed with aluminum tape to induce one-dimensional moisture transport. Two specimens of each material type were sampled at specified times within each cycle. Immediately upon removal from the climate chamber, 18 mm was cut from each edge with a table saw, achieving final specimen size of 38 by 38 mm. Next, the outer and inner veneers in plywood and the faces and core of OSB were isolated with a heavy-duty slicer. Bondlines in plywood granted easy visual identification of the veneer boundaries. The face and core of OSB were visually identified based on strand consolidation and alignment, which varied somewhat on a specimen basis. Each region was weighed immediately after slicing and then oven-dried to determine average gravimetric MC over each region.

The entire procedure from removing the specimen from the climate chamber to obtaining the mass of each region required less than 5 minutes. Some moisture exchange occurred within the laboratory environment during the MC specimen preparation. Specimens from the same population as those used in the experiments were prepared in the same manner to estimate the impact of moisture exchange on the MC value by recording the mass change of both unsliced and sliced specimens at 1-minute intervals for 5 minutes after they had been brought to equilibrium at 30°C and 30 or 90 percent RH.

Results and Discussion

Sorption isotherms

Nelson's sorption model fit the experimental data well, with R^2 ranging from 0.93 to 0.99 (Table 1). Sorption hysteresis was present for both materials; that is, EMC was significantly greater in desorption (analysis of variance $P \ll 0.0001$). The adsorption to desorption EMC ratios (A/D) for both material types (Table 1) were within the ranges of previously reported values (Skaar 1988, Wu and Ren 2000, Hartley et al. 2007). Instantaneous responses to boundary condition changes were not anticipated during the experimental RH cycling procedure used to assess model suitability. Therefore, regression analysis considering both adsorption and desorption data for each material was performed with the purpose of obtaining the combined adsorption/desorption isotherm (Table 1).

Moisture transport coefficients

The diffusion coefficient increased with MC for veneer (Table 2), and the values were within the range of those reported for softwood (Wadsö 1993, Siau 1995b, Cai and Avramidis 1997, Olek et al. 2005, Mannes et al. 2009). Consistent with past studies investigating mat-formed wood composites (Wu and Suchsland 1996, Ganev et al. 2003, Shi 2007), D of OSB face and core decreased with increasing MC (Table 2). Timusk (2008) determined that water vapor permeability differed significantly between layers of commercial OSB evaluated using steady-state cup experiments, which was attributed to greater thermal modification of the face during hot-pressing and subsequent density differences. In the current study, however, D differed only 6 percent between core and face when averaged over all sorption steps. The surface emission coefficient did not vary systematically as a function of MC for any material evaluated but tended to be greater in desorption (Table 2), which is consistent with past work (Siau and Avramidis 1996).

Average C over each step was computed by substituting the corresponding concentration terms in for MC at two-thirds the distance between starting and ending values for each step (Siau 1995b), and Equation 4 was used to determine concentration dependence of D considering adsorption and desorption separately (Table 3). For the purpose of modeling short-term cyclic changes in RH, an immediate change in the diffusion behavior, in terms of sorption direction, is likely not realized. Therefore, regression analysis was also performed for all adsorption and desorption points, which was considered as the combined data (Table 3).

The diffusion coefficient of adhesive used in plywood manufacture (D_{adh}) was estimated as 2.02 by 10^{-11} m^2 s^{-1} (Way 2018). A parametric sweep was performed in COMSOL Multiphysics to determine the MC gradient across the bondline under the steady-state cup conditions when D_{adh} ranged from 2.5 to 89.0 by 10^{-12} m^2 s^{-1}. The lower bound was chosen as that provided in literature for PRF (Sonderegger et al. 2010), while the upper bound was chosen as the value computed for the unbonded specimens during the experiment. The range of values was then input into the model during parametric analysis to determine which D_{adh} value produced the best agreement with experimental data.

Model agreement

RH measured in the climate chamber during the three-cycle sorption procedure was logged every minute and supplied to the model as a series of continuous linear segments (Fig. 1). One interruption to the chamber

Table 1.—Sorption isotherm parameter estimates for adsorption, desorption, and combined data, and A/D range.[a] *Values in parentheses are standard deviations.*

	Adsorption			Desorption			Combined			
Material[b]	M_v (-)	A (J g^{-1})	R^2	M_v (-)	A (J g^{-1})	R^2	M_v (-)	A (J g^{-1})	R^2	A/D range
Veneer	0.279 (0.004)	6.00 (0.05)	0.98	0.275 (0.005)	6.54 (0.07)	0.97	0.277 (0.005)	6.26 (0.06)	0.93	0.74–0.84
OSB face	0.307 (0.005)	5.82 (0.04)	0.97	0.297 (0.002)	6.50 (0.03)	0.99	0.302 (0.006)	6.14 (0.06)	0.93	0.68–0.82
OSB core	0.302 (0.004)	5.86 (0.04)	0.98	0.293 (0.003)	6.51 (0.04)	0.99	0.297 (0.005)	6.16 (0.04)	0.94	0.71–0.83

[a] Ratio of equilibrium moisture content in adsorption to desorption.
[b] OSB = oriented strand board.

Table 2.—*Diffusion coefficient (*D*), surface emission coefficient (*S*), and objective function value (*F*) for each sorption step.*[a]

Material	Sorption step (% RH)	$\bar{M}$ (%)[b]	D ($m^2\ s^{-1} \times 10^{-11}$)	S ($m\ s^{-1} \times 10^{-8}$)	F ($\times 10^{-3}$)
Veneer	30 → 45	5.4	15.9	7.3	13.10
	45 → 60	6.8	24.1	2.0	9.33
	60 → 75	9.6	30.5	1.8	4.97
	75 → 90	14.0	49.9	2.2	4.23
	90 → 75	14.7	38.0	8.4	7.84
	75 → 60	11.9	28.0	7.8	12.6
	60 → 45	9.0	13.4	8.3	7.19
	45 → 30	6.7	11.6	8.5	8.35
OSB core	30 → 45	5.4	10.6	30.9	9.26
	45 → 60	6.9	7.7	9.0	9.38
	60 → 75	9.7	3.0	17.0	3.73
	75 → 90	14.7	3.5	22.5	0.82
	90 → 75	15.5	7.9	27.6	6.70
	75 → 60	12.2	9.1	23.5	7.59
	60 → 45	9.7	9.4	19.0	3.89
	45 → 30	7.4	9.9	25.0	4.08
OSB face	30 → 45	5.3	8.5	4.3	15.40
	45 → 60	6.8	5.5	2.5	9.00
	60 → 75	9.7	3.2	2.9	5.11
	75 → 90	14.9	2.5	6.6	1.84
	90 → 75	15.7	8.0	9.8	8.71
	75 → 60	12.3	11.6	5.4	12.20
	60 → 45	9.7	12.2	6.0	5.09
	45 → 30	7.5	13.7	6.3	8.90

[a] RH = relative humidity; OSB = oriented strand board.
[b] Moisture content at two-thirds sorption over RH step.

operation occurred from brief loss of power, which increased RH around 90 hours (Fig. 1) before the chamber was restored back to set point 1 hour later. Sixteen sampling points occurred during the three-cycle procedure, which generally occurred at 6, 18, and 23.75 hours into each step (Fig. 1). Global relative error (e) was used to compare the average MC measured for each layer during the experiment and that predicted by the model (Olek et al. 2005) as:

$$e = \frac{\sqrt{\sum_{i=1}^{N}\left[\mathrm{MC}_{\exp}(t_i) - \mathrm{MC}_{\mathrm{pred}}(t_i)\right]^2}}{\sqrt{\sum_{i=1}^{N}\mathrm{MC}_{\exp}(t_i)^2}} \cdot 100 \qquad (6)$$

Table 3.—*Regression parameters for concentration-dependent* D *in each sorption direction.*[a]

Material[b]	Regression parameters	Sorption direction		
		Adsorption	Desorption	Combined
Veneer	D_0	0.94	0.18	0.58
	α	0.021	0.038	0.026
	R^2	0.97	0.90	0.98
OSB core	D_0	1.92	1.20	1.55
	α	−0.025	−0.005	−0.014
	R^2	0.72	0.86	0.85
OSB face	D_0	1.49	2.16	1.77
	α	−0.019	−0.008	−0.011
	R^2	0.82	0.86	0.99

[a] D_0 ($m^2\ s^{-1} \times 10^{-10}$), α ($m^3\ kg^{-1}$).
[b] OSB = oriented strand board.

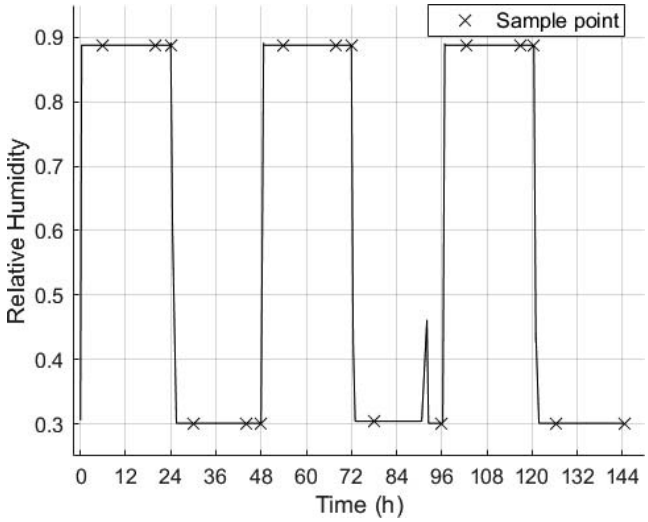

Figure 1.—Relative humidity inputs for experimental moisture cycling and sampling points.

The best agreement between average MC of each layer considering all sampling points and that predicted by the model for OSB resulted in e of 6.6, 11.4, and 9.0 percent for the face layer, core layer, and the face and core layer combined, respectively. The best agreement occurred when using the combined sorption isotherm (Table 1), separate average S for each sorption direction (Table 4), and concentration-dependent D, based on the regression equation for adsorption and desorption combined, in both face and core (Table 3). Comparison between the modeled and predicted values for this combination of model inputs is shown in Figure 2. The prediction error was relatively consistent across the three cycles for the face layer but increased with each cycle for the core layer (Fig. 2). Error for the core layer was greatest during the low humidity steps, where the model tended to predict greater moisture accumulation than realized in the experimental determination, particularly at the end of the third cycle (Fig. 2). Linear regression of the predicted versus measured MC values for both the face and core across all sampling points showed reasonable agreement with a correlation coefficient (R^2) of 0.87.

The best agreement between average MC of each layer considering all sampling points and that predicted by the model for plywood resulted in e of 11.2, 9.2, and 10.2 percent for the outer layer, inner layer, and both layer types combined, respectively. The combination of parameters producing the lowest error was: sorption isotherm for adsorption and desorption data combined (Table 1), S applied separately for each sorption direction (Table 4),

Table 4.—*Average* S *in adsorption, desorption, and all sorption steps.*

Material[a]	S ($m\ s^{-1} \times 10^{-8}$)		
	Adsorption	Desorption	All[b]
Veneer	3.33	8.25	5.79
OSB face	4.08	6.88	5.48

[a] OSB = oriented strand board.
[b] Average for all adsorption and desorption measurements.

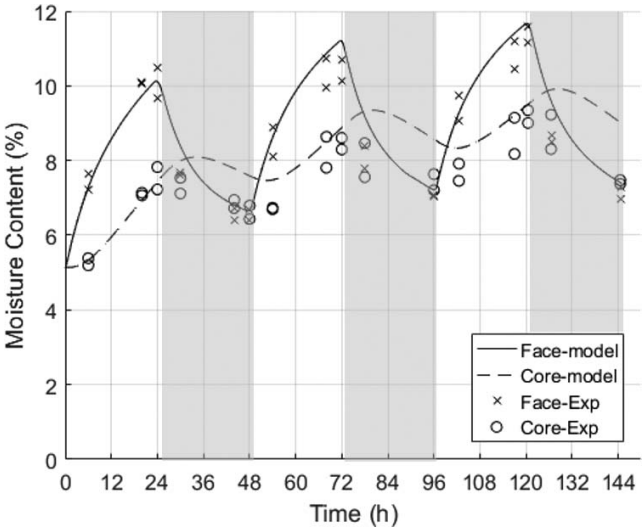

Figure 2.—Measured (Exp) and predicted (model) average moisture content of oriented strand board face and core layers over three cycles. Times within shaded regions represent the 30 percent relative humidity steps.

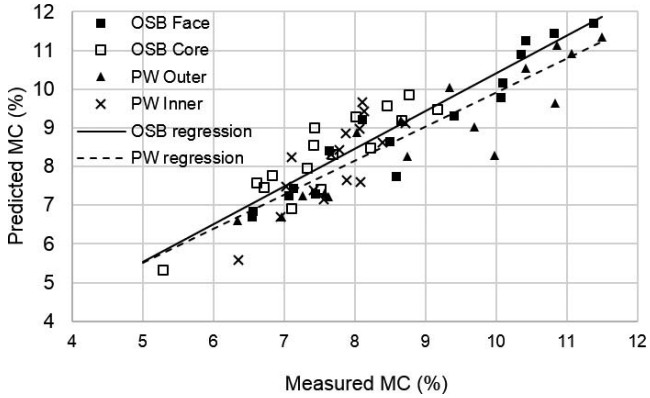

Figure 3.—Moisture content (MC) predicted by the model versus measured MC for each oriented strand board (OSB) and plywood (PW) layer.

combined moisture concentration-dependent D for veneer (Table 3), and D_{adh} of 9.5 by 10^{-12} m^2 s^{-1}. Comparison between the modeled and predicted values for this combination of model inputs is shown in Figure 3. Prediction error was greatest during the first cycle and decreased with each subsequent cycle (Fig. 4). Outer layer MC tended to underpredict, while MC of the inner layer was underpredicted during the first cycle and slightly overpredicted for the remaining cycles (Fig. 4). As the e values indicated, the plywood model did not fit the experimental data as well as the OSB model, which was verified with linear regression of the predicted versus measured MC of the outer and inner plywood layers at each sampling point (Fig. 3) yielding $R^2 = 0.75$.

The procedure to determine deviation in MC caused by moisture exchange with the laboratory environment indicated that the maximum deviation always occurred with sliced specimens. For OSB, the largest deviation would result in maximum errors of 0.2 and –0.5 percent MC when preparing during the low and high humidity steps, respectively. Applying these estimation errors to the measured MC values resulted in a slight improvement to predicted versus measured average MC values, with $R^2 = 0.88$ compared to $R^2 = 0.87$ without compensating for moisture exchange during specimen preparation. For plywood, the largest deviation would result in maximum errors of 0.3 and –0.6 percent MC when preparing during the low and high humidity steps, respectively. Application of these adjustments decreased the fit of predicted versus measured values from $R^2 = 0.75$ to $R^2 = 0.72$.

The experimental and modeling methodology was chosen due to ease of implementation and relatively simple, readily available experimental procedure, meaning it could be more easily adapted by the wood-based composites industry. An average deviation of 9.0 and 10.2 percent over three cycles for OSB and plywood, respectively, indicated that the simple model, while not perfect, could largely capture the general trends of moisture transport during cyclic changes in RH at isothermal conditions. The consistent rise in error for the OSB core layer with increasing cycles indicated that limitations exist as to how many cycles can be evaluated with this modeling methodology—which likely stems from the acknowledged inadequacies of assuming single-phase Fickian diffusion combined with the unsophisticated transport coefficient measurement technique. In addition, the manual slicing technique and natural differences between multiple specimens evaluated throughout the experimental procedure could introduce additional sources of error.

Model application

The primary objective of this work was to determine whether a relatively simple Fickian diffusion model could be used to reasonably predict MC in OSB and plywood under cyclic RH conditions, which could be implemented as a potential AW procedure. The method of obtaining MC values experimentally (i.e., slicing) limits evaluating measured and predicted data to average MC of each layer. Moisture gradients within the specimen are of most interest

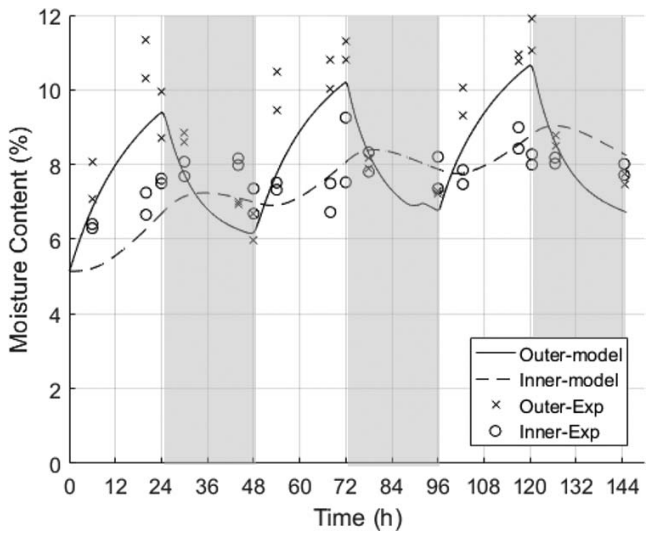

Figure 4.—Measured (Exp) and predicted (model) average moisture content for plywood outer and inner veneers. Times within shaded regions represent the 30 percent relative humidity steps.

during AW. The reasonable model fit along with the ability to predict the general trends would indicate that the model should be able to roughly estimate moisture gradients throughout the depth. Simulations were performed to investigate deviations in the chosen experimental procedure. The RH cycling procedure for model validation consisted of three cycles, where each cycle had a high RH step (90%) and low RH step (30%) with 24-hour duration each. The influence of step length on average MC for each layer and moisture gradient formation was investigated with two additional simulations, where the same RH conditions were used but the step length was extended to either 48 or 72 hours. For each case, RH was assumed to increase or decrease linearly between 30 and 90 percent RH for 30 minutes after the conditions changed.

The internal MC gradients in OSB were determined by dividing the entire section into four regions of equal thickness, where symmetry about middle thickness was assumed. Each region was set to 1.4 mm thick and was numbered sequentially beginning at the exposed face layer surface. The moisture gradient was computed as the difference between the maximum and minimum MC across the region, referred to as the maximum differential MC (MDMC). In plywood, the primary location of interest in terms of moisture gradients was across the bondline. The MC difference across the bondline (MCDBL) was computed as the difference between MC at the location of the outer veneer immediately adjacent to the bondline and the MC at the location of the inner veneer immediately adjacent to the bondline.

Peak average MC in the OSB face, which occurred during the high humidity steps, increased with each cycle (Fig. 5), which indicated that moisture accumulation occurred for all step times. However, moisture accumulation in the face decreased with increasing step time (Fig. 5). Peak average MC in the core also increased with each cycle; however, the time at which the peak MC occurred was offset from the face and happened in the low humidity step (Fig. 5). The length of time into the desorption step at which peak average core MC occurred decreased with increasing step time (Fig. 5). The largest MDMCs occurred in the first region (Fig. 6) of the face shortly into each high humidity step for all step times; however, while the greatest MDMC was achieved during the first high humidity step, it decreased with each additional cycle (Fig. 6). MDMC in the other face region (Fig. 6) remained relatively small compared with the first region, reaching approximately half the peak value. MDMC of the core regions (Fig. 6) remained small at less than 1.0 percent MC.

Extending the step time to 48 or 72 hours had little influence on maximum MDMC during the high RH steps (Fig. 6). During the low RH steps, however, the influence of step time on MDMC was apparent. Formation of relatively high MDMC in region 1 was seen during low humidity steps regardless of step time. However, for 24 hours step time, the MDMC during low humidity did not reach similar levels to those during high humidity until the second and third cycles. Extending the step length to 48 or 72 hours produced MDMC in region 1 during low humidity steps at similar or higher levels than during high humidity, which was present during all cycles (Fig. 6b,c).

The maximum and minimum average MC for plywood in the outer veneer always occurred at the end of the high and low humidity steps, respectively, regardless of step length

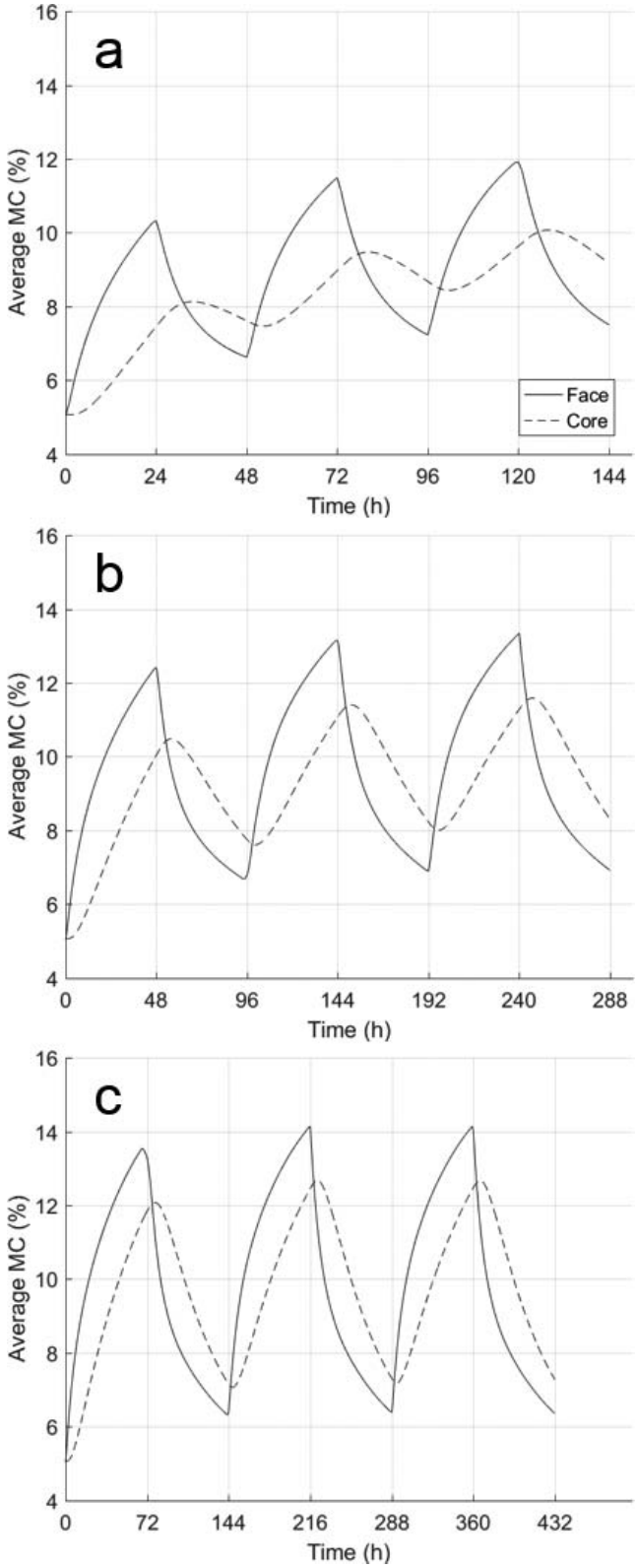

Figure 5.—Average moisture content (MC) for face and core layers for simulations with step times of (a) 24, (b) 48, and (c) 72 hours. Note: legend in (a) applies to (a–c).

(Fig. 7). Moisture accumulation throughout the procedure was evident with the maximum average MC of both layers increasing each cycle, but the effect was lessened as cycle time increased (Fig. 7). The greatest MCDBL occurred

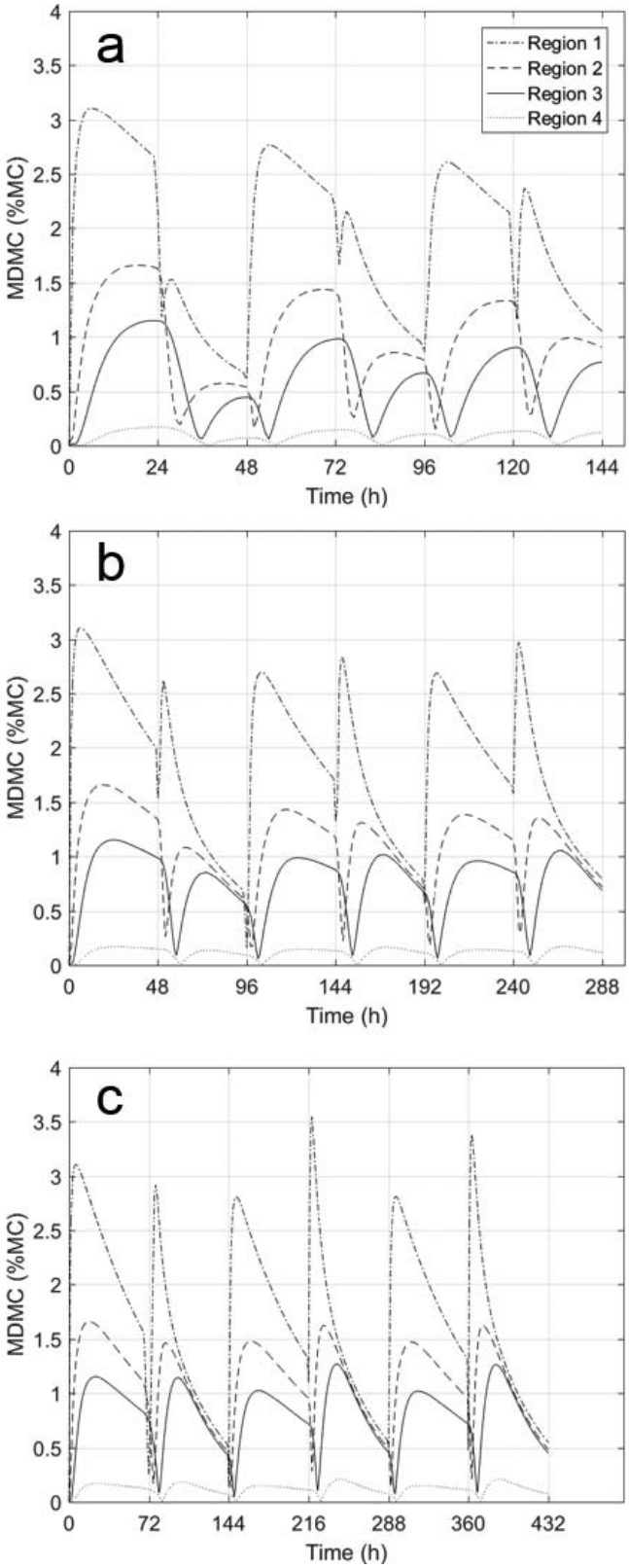

Figure 6.—Maximum differential moisture content (MDMC) for the four oriented strand board regions for simulations with step times of (a) 24, (b) 48, and (c) 72 hours. Note: legend in (a) applies to (a–c).

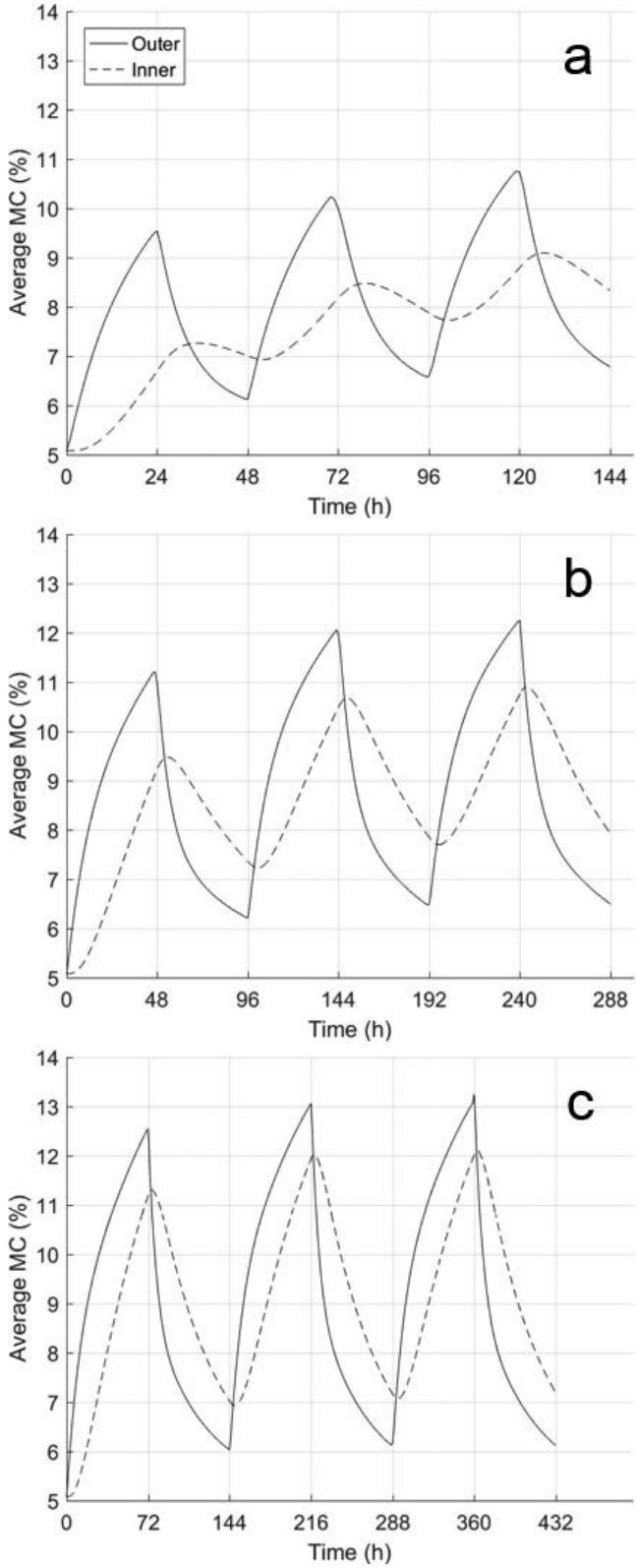

Figure 7.—Average moisture content (MC) for outer and inner veneers for simulations with step times of (a) 24, (b) 48, and (c) 72 hours. Note: legend in (a) applies to (a–c).

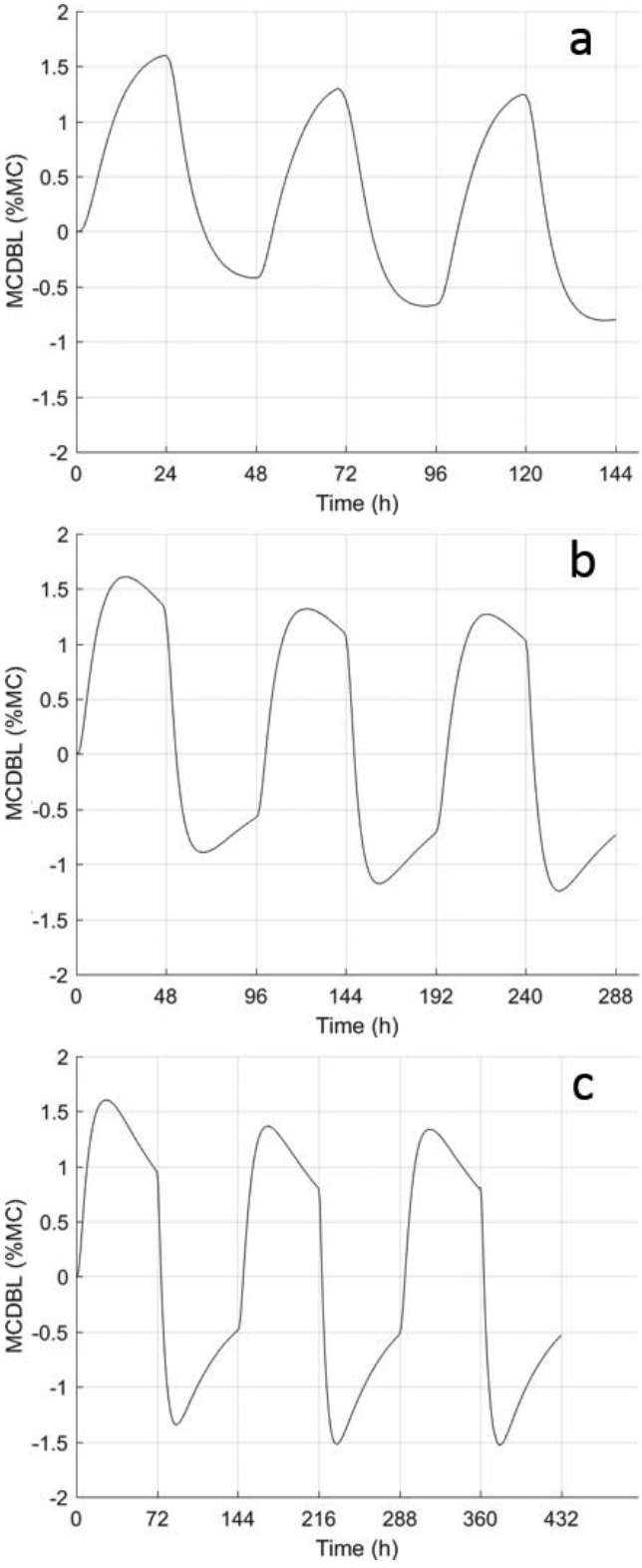

Figure 8.—The moisture content difference across the bondline (MCDBL) for simulations with step times of (a) 24, (b) 48, and (c) 72 hours.

during the first high RH step regardless of step time, and the maximum MCDBL reached during high humidity decreased for cycles 2 and 3 (Fig. 8). The gradient at the bondline gradually decreased as RH switched from high to low and eventually changed direction, resulting in the inner veneer adjacent to the bondline having higher MC than that of the outer veneer (i.e., negative MCDBL, Fig. 8). The 24-hour step time resulted in relatively small negative MCDBL (Fig. 8a). Extending the step time, however, resulted in greater negative MCDBL values at a similar level to those occurring during the high humidity steps (Figs. 8b and 8c).

Conclusions

A simple method to predict MC in wood-based panels during RH cycling at constant temperature was evaluated for the purpose of providing practitioners lacking sophisticated modeling and measurement equipment a means of evaluating less severe AW procedures. A simple single-phase diffusion model based on Fick's second law, with empirically determined transport properties, was tested against experimental RH cycling data.

It was found that while not perfect, the model was capable of capturing the general trends of moisture transport through the thickness of OSB and plywood during cyclic RH exposure. The procedure could be used by members of the wood-based composites industry to estimate moisture transport in OSB and plywood, along with the impact of cycle lengths, when developing RH cycling AW procedures.

Acknowledgments

Financial support was provided by the Wood-Based Composites Center, a National Science Foundation (NSF) Industry/University Cooperative Research Center (Project No. IIP-1624599).

Literature Cited

APA. 2011. PS 2-10: Performance standard for wood-based structural-use panels. APA—The Engineered Wood Association, Tacoma, Washington.

APA. 2018. PRP-108: Performance standards and qualification policy for wood structural panels. APA—The Engineered Wood Association, Tacoma, Washington.

ASTM International. 2012. Standard test methods for evaluating properties of wood-base fiber and particle panel materials. ASTM D1037. ASTM International, West Conshohocken, Pennsylvania.

Cai, L. and S. Avramidis. 1997. A study on the separation of diffusion and surface emission coefficients in wood. *Dry Technol*. 15:1457–1473.

COMSOL. 2015a. COMSOL Multiphysics, version 5.1. COMSOL AB, Stockholm. www.comsol.com. Accessed July 3, 2018.

COMSOL. 2015b. COMSOL Multiphysics User Guide, version 5.1. COMSOL AB, Stockholm.

Crank, J. 1986. The Mathematics of Diffusion. 2nd ed. Clarendon Press, Oxford, UK.

Eitelberger, J. and K. Hofstetter. 2011. Prediction of transport properties of wood below the fiber saturation point—A multiscale homogenization approach and its experimental validation. Part 1: Thermal conductivity. *Compos. Sci. Technol*. 71:134–144.

Frandsen, H. L., L. Damkilde, and S. Svensson. 2007. A revised multi-Fickian moisture transport model to describe non-Fickian effects in wood. *Holzforschung* 61:563–572. DOI:10.1515/HF.2007.085

Ganev, S., A. Cloutier, R. Beauregard, and G. Gendron. 2003. Effect of panel moisture content and density on moisture movement in MDF. *Wood Fiber Sci*. 35:68–82.

Ganev, S., A. Cloutier, G. Gendron, and R. Beauregard. 2005. Finite element modeling of the hygroscopic warping of medium density fiberboard. *Wood Fiber Sci*. 37:337–354.

Gereke, T. 2009. Moisture-induced stresses in cross-laminated wood panels. PhD dissertation. Swiss Federal Institute of Technology, Zürich.

Hartley, I., S. Wang, and Y. Zhang. 2007. Water vapor sorption isotherm

modeling of commercial oriented strand panel based on species group and resin type. *Build. Environ*. 42:3655–3659.
Hassani, M. M., F. K. Wittel, and S. Ammann. 2016. Moisture-induced damage evolution in laminated beech. *Wood Sci. Technol*. 50:917–940. DOI:10.1007/s00226-016-0821-5
Mannes, D., S. Sanabria, and M. Funk. 2014. Water vapour diffusion through historically relevant glutin-based wood adhesives with sorption measurements and neutron radiography. *Wood Sci. Technol*. 48:591–609. DOI:10.1007/s00226-014-0626-3
Mannes, D., W. Sonderegger, and S. Hering. 2009. Non-destructive determination and quantification of diffusion processes in wood by means of neutron imaging. *Holzforschung* 63:589–596. DOI:10.1515/HF.2009.100
Moya, L., W. T. Tze, and J. E. Winandy. 2009. The effect of cyclic relative humidity changes on moisture content and thickness swelling behavior of oriented strandboard. *Wood Fiber Sci*. 41:447–460.
Nelson, R. M. 1983. A model for sorption of water vapor by cellulosic materials. *Wood Fiber Sci*. 15:8–22.
Niklewski, J., M. Fredriksson, and T. Isaksson. 2016. Moisture content prediction of rain-exposed wood: Test and evaluation of a simple numerical model for durability applications. *Build. Environ*. 97:126–136.
Olek, W., P. Perré, and J. Weres. 2005. Inverse analysis of the transient bound water diffusion in wood. *Holzforschung* 59:38–45. DOI:10.1515/HF.2005.007
River, B. H. 1994. Outdoor aging of wood-based panels and correlation with laboratory aging. *Forest Prod. J*. 44(11/12):55–65.
Saad, S., H. Kobori, Y. Kojima, and S. Suzuki. 2016. Performance evaluation of wood-based panels under a mild accelerated aging treatment. *J. Wood Sci*. 62:324–331. DOI:10.1007/s10086-016-1564-5
Saft, S. and M. Kaliske. 2011. Numerical simulation of the ductile failure of mechanically and moisture loaded wooden structures. *Comput. Struct*. 89:2460–2470. DOI:10.1016/j.compstruc.2011.06.004
Shi, S. 2007. Diffusion model based on Fick's second law for the moisture absorption process in wood fiber-based composites: Is it suitable or not? *Wood Sci. Technol*. 41:645–658. DOI:10.1007/s00226-006-0123-4
Siau, J. F. 1995a. Chapter 8: Unsteady-state transport, mass convection, and nonisothermal diffusion. *In:* Wood: Influence of Moisture on Physical Properties. J. F. Siau (Ed.). Department of Wood Science and Forest Products, Virginia Polytechnic Institute and State University, Blacksburg. pp. 143–188.
Siau, J. F. 1995b. Chapter 6: Steady-state moisture diffusion. *In:* Wood: Influence of Moisture on Physical Properties. J. F. Siau (Ed.). Department of Wood Science and Forest Products, Virginia Polytechnic Institute and State University, Blacksburg p. 112.
Siau, J. F. and S. Avramidis. 1996. The surface emission coefficient of wood. *Wood Fiber Sci*. 28(2):178–185.
Skaar, C. 1988. Wood-Water Relations. Springer-Verlag, Berlin.
Sonderegger, W., S. Hering, and D. Mannes. 2010. Quantitative determination of bound water diffusion in multilayer boards by means of neutron imaging. *Eur. J. Wood Wood Prod*. 68:341–350. DOI:10.1007/s00107-010-0463-5
Timusk, P. C. 2008. An investigation of the moisture sorption and permeability properties of mill-fabricated oriented strandboard. PhD dissertation. University of Toronto.
Wadsö, L. 1993. Measurements of water vapour sorption in wood: Part 2. Results. *Wood Sci. Technol*. 28:59–65.
Way, D. 2018. Multi-scale approach to evaluating moisture durability of wood-based composites. PhD dissertation. Oregon State University, Corvallis. https://ir.library.oregonstate.edu/concern/graduate_thesis_or_dissertations/jw827j042. Accessed August 19, 2018.
Wimmer, R., O. Kläusler, and P. Niemz. 2013. Water sorption mechanisms of commercial wood adhesive films. *Wood Sci Technol*. 47:763–775. DOI:10.1007/s00226-013-0538-7
Wu, Q. and Y. Ren. 2000. Characterization of sorption behavior of oriented strandboard under long-term cyclic humidity exposure condition. *Wood Fiber Sci*. 32(4):404–418.
Wu, Q. and O. Suchsland. 1996. Prediction of moisture content and moisture gradient of an overlaid particleboard. *Wood Fiber Sci*. 28(2):227–239.